

Towards Compatible Fine-tuning for Vision-Language Model Updates

Zhengbo Wang^{1,2}, Jian Liang^{2,3}*, Lijun Sheng^{1,2}, Ran He^{2,3}, Zilei Wang¹, Tieniu Tan^{2,3,4}

¹ University of Science and Technology of China

² NLPR & MAIS, Institute of Automation, Chinese Academy of Sciences

³ School of Artificial Intelligence, University of Chinese Academy of Sciences

⁴ Nanjing University

zhengbowang@mail.ustc.edu.cn, liangjian92@gmail.com

Abstract

So far, efficient fine-tuning has become a popular strategy for enhancing the capabilities of foundation models on downstream tasks by learning plug-and-play modules. However, existing methods overlook a crucial issue: *if the underlying foundation model is updated, are these plug-and-play modules still effective?* In this paper, we first conduct a detailed analysis of various fine-tuning methods on the CLIP in terms of their compatibility with model updates. The study reveals that many high-performing fine-tuning methods fail to be compatible with the upgraded models. To address this, we propose a novel approach, **Class-conditioned Context Optimization (ContCoOp)**, which integrates learnable prompts with class embeddings using an attention layer before inputting them into the text encoder. Consequently, the prompts can dynamically adapt to the changes in embedding space (due to model updates), ensuring continued effectiveness. Extensive experiments over 15 datasets show that our ContCoOp achieves the highest compatibility over the baseline methods, and exhibits robust out-of-distribution generalization.

1 Introduction

In the current era, foundation models [Radford et al., 2021, Kenton and Toutanova, 2019, Brown et al., 2020, Rombach et al., 2022, Caron et al., 2021] have emerged as the cornerstone of the field of deep learning. Through pre-training on exceptionally large datasets, these models demonstrate remarkable zero-shot capabilities and generalization, rendering them extensively employed across various domains.

Efficient fine-tuning has emerged as a prominent area of research in the context of large foundation models [Zhou et al., 2022b,a, Hu et al., 2022, Li and Liang, 2021, Houlsby et al., 2019]. By freezing the parameters of foundation models, these approaches train lightweight plug-and-play modules to quickly and cost-effectively adapt the model to downstream tasks, such as learning residual matrices [Hu et al., 2022, Dettmers et al., 2023] or additional learnable prompts [Zhou et al., 2022b, Li and Liang, 2021, Houlsby et al., 2019]. Consequently, by maintaining a frozen large model alongside corresponding lightweight modules, we can low-costly apply the foundation model to thousands of downstream tasks.

The existing efficient fine-tuning methods neglect a crucial problem. To improve model performance or attain a safety alignment [Ouyang et al., 2022, Sun et al., 2023, Xu et al., 2023, Touvron et al., 2023, Chiang et al., 2023, Rombach et al., 2022], the foundational models at the core are often updated, such as the transition from GPT-3 to ChatGPT, CLIP to EVA-CLIP, and the series of versions in stable diffusion. However, prior to model updates, we have trained a variety of plug-and-play modules on the current version of the foundation model. This raises a significant question:

*Correspondence to: Jian Liang (liangjian92@gmail.com)

*Can these efficient fine-tuning modules be compatible
with the upgraded foundation model?*

Given the substantial costs associated with retraining numerous plug-in modules, exploring the compatibility of these modules emerges as a meaningful pursuit.

We investigate the compatibility of efficient fine-tuning methods on vision-language models (VLMs) in the context of model upgrades. Such methods can be categorized into two types: one involves adding learnable prompts at the model’s shallow layers, while the other entails incorporating learning modules to refine the text features at the model’s deep layers. The latter methods generally exhibit superior performance when applied to downstream tasks.

We first investigate the compatibility of existing methods. We train these plug-and-play modules on CLIP and directly integrate them into the upgraded model, EVA-CLIP. The results reveal an interesting observation: while deep-layer fine-tuning methods demonstrate superior performance, their compatibility to updated models falls short, even performing worse than the zero-shot performance of the upgraded model. Consequently, we posit that, for the model upgrade of VLMs, the shallow layers exhibit better transferability compared to the deeper layers.

To delve deeper into this phenomenon, we compute the average absolute and relative changes between parameters and output features for each layer before and after model upgrades. The analysis reveals that the changes in shallower layers are consistently smaller, confirming the better transferability of these layers. To address potential concerns related to methodological influences, we conduct additional experiments. Specifically, we train CoOp [Zhou et al., 2022b] at different layers. The results consistently show a decline in reused performance with increasing layer depth, providing empirical support for our hypothesis.

To address the problem, we propose a novel approach, **Class-conditioned Context Optimization (ContCoOp)**, designed to enhance compatibility. Our approach involves learning class-conditioned prompts at the input of the text encoder, akin to shallow-layer methods. Prior to inputting into the text encoder, we integrate class information into the learnable prompts through an attention network. Consequently, these prompts possess the capability to dynamically evolve alongside updates to the class embedding within the enhanced model. This dynamic adaptability significantly enhances the compatibility of the prompts in upgraded models.

Our contributions are summarized as follows:

- To the best of our knowledge, this paper is the first work exploring the module compatibility problem in VLMs. Given the high cost associated with re-training the fine-tuning modules after model updates, investigating fine-tuning methods with strong compatibility in upgraded models becomes imperative.
- We assess the compatibility of existing efficient fine-tuning methods in VLMs for model upgrades. Our study reveals an interesting observation: shallower layers demonstrate superior transferability compared to deeper layers. This discovery can potentially enhance the design of fine-tuning methods in the future.
- We propose a novel approach named **Class-conditioned Context Optimization (ContCoOp)**. Leveraging an attention network, we obtain class-conditioned prompts for downstream tasks, allowing for dynamic updates to accommodate the improved model, thereby enhancing compatibility.

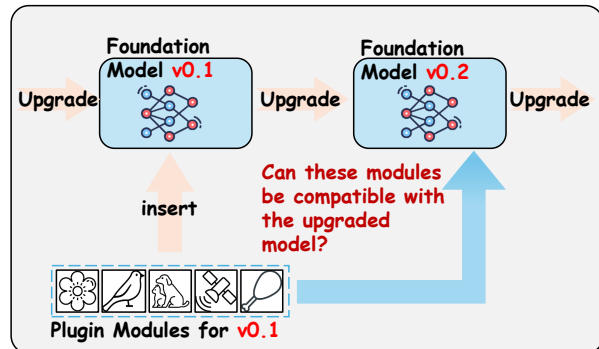


Figure 1: Efficient fine-tuning methods enable us to easily train plug-and-play modules to enhance the performance of foundation models. However, a significant challenge arises due to the frequent updates in foundational models, such as variants of Llama and CLIP. Re-training these modules for the upgraded model incurs significant costs. Therefore, our investigation aims to address the question of *whether these modules can be compatible with the upgraded model*.

	ZS-CLIP (ICML'21)	LP† (ICML'21)	CLIP-A† (IJCV'23)	Tip-A† (ECCV'22)	CoOp (IJCV'22)	CoCoOp (CVPR'22)	KgCoOp (CVPR'23)
Base	65.51	78.15	79.56	81.63	79.94	76.27	78.30
New	70.79	1.83	67.30	69.63	75.40	75.39	75.77
H	68.04	3.57	72.92	75.15	77.60	75.83	77.01

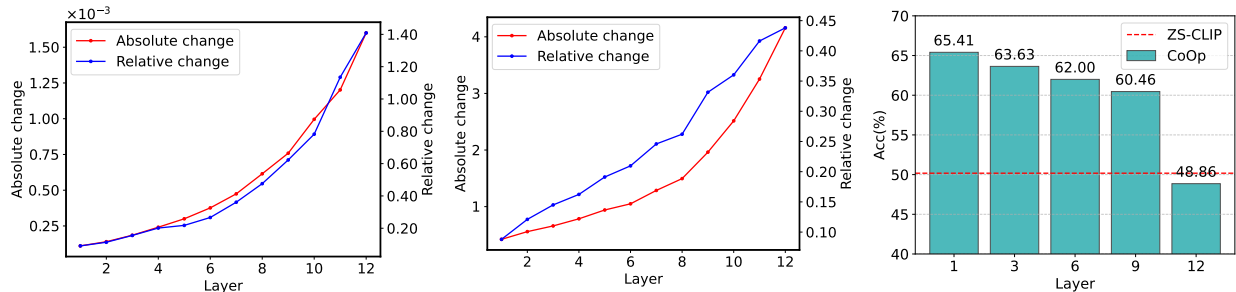


Figure 2: (a) The average performance over 11 datasets. We assess the compatibility of efficient fine-tuning methods of VLMs for model upgrades. These methods are trained on ViT-B/16-based CLIP and then integrated into the corresponding EVA-CLIP, the upgraded model. The terms Base and New represent the performance tested after inserting these modules into CLIP and EVA-CLIP, with H indicating their harmonic average. † denotes that is a deep-layer method. (b) The average absolute and relative changes in parameters at each layer of the text encoder before and after model upgrading. (c) The average absolute and relative changes in output features at each layer of the text encoder before and after model upgrading. (d) To mitigate methodological impacts, we train CoOp at different layers on the DTD dataset and report its accuracy on the upgraded model. The results indicate that shallower layers exhibit superior transferability compared to deeper layers.

- We conduct extensive experiments over 15 datasets, which shows that our method exhibits superior compatibility compared to the baseline methods.

2 Related Work

Vision-Language Models. Vision-Language Models (VLMs) have emerged as a new kind of foundation model, aiming to connect vision and language modalities [Radford et al., 2021, Kim et al., 2021, Lu et al., 2019, Su et al., 2019, Jia et al., 2021, Sun et al., 2023, Cherti et al., 2023, Li et al., 2023]. Trained on extensive image-text datasets, these models showcase remarkable zero-shot recognition and generalization capabilities and they have been widely applied in open-world recognition [Joseph et al., 2021, Gu et al., 2021, Liang et al., 2023] and text-to-image generation [Rombach et al., 2022, Ramesh et al., 2021, 2022]. In this paper, our focus is on CLIP [Radford et al., 2021] and its upgraded version, EVA-CLIP [Sun et al., 2023]. Both models are composed of an image encoder and a text encoder, trained with a contrastive loss to align representations from different modalities. EVA-CLIP leverages the pre-trained text encoder of CLIP and undergoes further contrastive learning on an improved visual model, ultimately showcasing superior performance.

Efficient Fine-Tuning for VLMs. To efficiently and cost-effectively adapt models to downstream tasks, recent research has concentrated on the development of effective fine-tuning methods within VLMs [Zhou et al., 2022b,a, Wang et al., 2023, Gao et al., 2023, Zhang et al., 2022, Yao et al., 2023, Wang et al., 2024, Shu et al., 2022]. These methods learn small plug-and-play modules that enhance the model by seamlessly integrating into the frozen model. Broadly, these methods can be categorized into two types based on the insertion position: shallow-layer and deep-layer methods. Shallow-layer methods [Zhou et al., 2022b,a, Wang et al., 2023], such as CoOp [Zhou et al., 2022b], focus on learning effective and robust prompts concatenating in

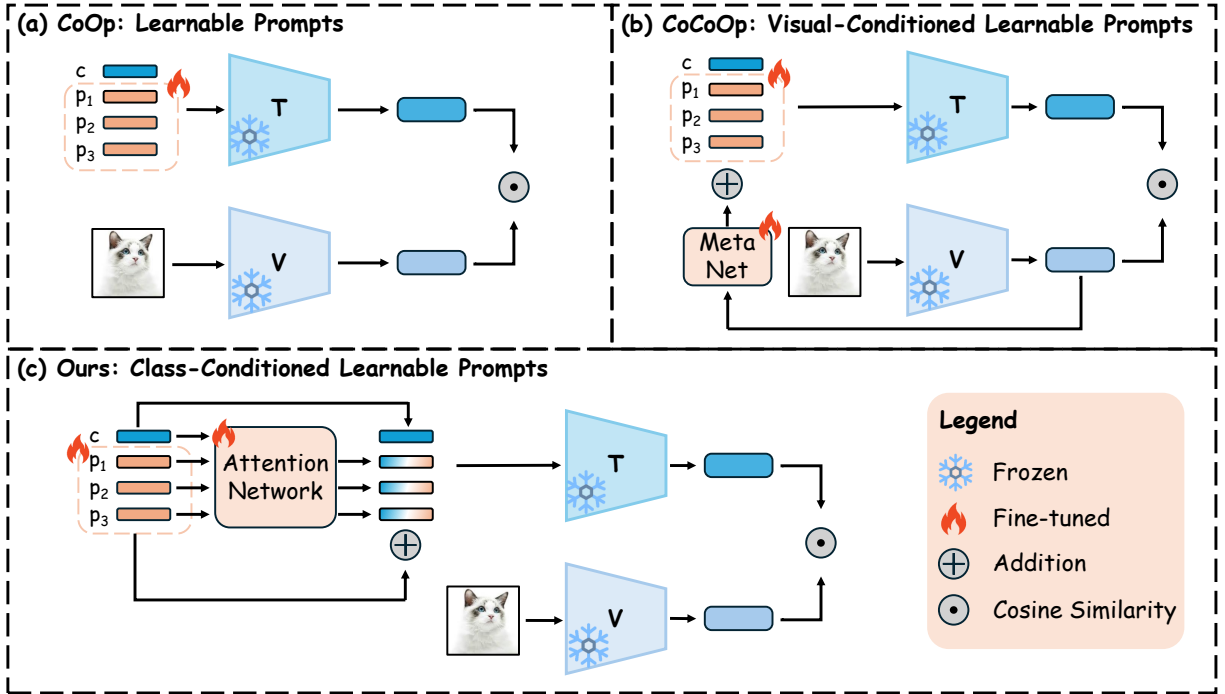


Figure 3: **The overview of our method.** To enhance the compatibility, we aim for our modules to dynamically adapt to model updates. For this, we adopt class-conditioned learnable prompts. Leveraging the attention network, our method integrates class information into learnable prompts. Moreover, following model updates, the prompts also undergo automatic updates, synchronized with changes in class embeddings. We include CoOp and CoCoOp for comparison.

the initial layer of the CLIP text encoder. In contrast, deep-layer methods [Zhang et al., 2022, Gao et al., 2023, Wang et al., 2024] learn to refine the output features with an adapter network or a cache model. While deep-layer methods typically exhibit superior performance on downstream tasks, our observation reveals that, in the context of adapting to updated models, shallow-layer methods demonstrate better compatibility. **Model Upgrades.** While foundation models exhibit strong performance and have been applied across various domains, continuous upgrades are essential to enhance their performance and achieve safety alignment [Touvron et al., 2023, Rombach et al., 2022, Sun et al., 2023, Ouyang et al., 2022]. In the field of NLP, model updates are ubiquitous. GPT-3, for instance, has evolved to ChatGPT through instruction fine-tuning and reinforcement learning with human feedback. The Llama series has undergone numerous upgrades through training on various datasets, resulting in versions such as Alpaca [Taori et al., 2023], Vicuna [Chiang et al., 2023], LLaVa [Liu et al., 2023], and more. Similarly, within the realm of generative models, frequent model upgrades are commonplace, exemplified by different versions of Stable Diffusion [Rombach et al., 2022]. In the domain of VLMs, model upgrades remain prevalent. For instance, CLIP [Radford et al., 2021] has been upgraded to the corresponding EVA-CLIP [Sun et al., 2023]. However, preceding these model upgrades, we have trained several plug-and-play fine-tuning modules. Retraining these modules after model updates incurs high costs. Due to limitations in computational resources, this paper predominantly investigates the module compatibility challenges in VLMs. We aim to devise an efficient fine-tuning method that exhibits robust compatibility for model updates in VLMs.

3 Method

3.1 Preliminary Study

In this paper, we concentrate on investigating the compatibility of efficient fine-tuning modules in VLMs for model updates. These efficient fine-tuning models are trained on the CLIP model, and we aim to explore their compatibility with the updated model, EVA-CLIP.

CLIP & EVA-CLIP. CLIP [Radford et al., 2021] and EVA-CLIP [Sun et al., 2023] are contrastive-based vision language models, comprising an image encoder I and a text encoder T for encoding inputs from their respective modalities. As these models have been trained on large-scale image-text pairs, we can easily obtain the zero-shot classifier weight $\{w_i\}_{i=1}^K$ through prompting, where $w_i = T(P_i)$, and P_i is the text prompt such as "a photo of a [class]" for i -th class. EVA-CLIP, an upgraded version of CLIP, leverages the text encoder from CLIP and further aligns it with an improved image encoder through training on image-text pairs. It exhibits superior performance compared to CLIP.

Can existing methods be compatible with the upgraded model? First, we investigate the compatibility of existing efficient fine-tuning methods for model updates. We assess the compatibility of six baselines: Linear Probe [Radford et al., 2021], CLIP-Adapter [Gao et al., 2023], Tip-Adapter [Zhang et al., 2022], CoOp [Zhou et al., 2022b], CoCoOp [Zhou et al., 2022a], and KgCoOp [Yao et al., 2023]. The first three are deep-layer methods, while the latter three are shallow-layer methods. We train these plug-and-play modules on ViT-16/B-based CLIP and evaluate their performance when integrated into CLIP and EVA-CLIP. We denote their performance on CLIP and EVA-CLIP as base and new, respectively, and report the harmonic mean (H) to balance these two metrics.

We report their average performance over 11 datasets at Figure 2 (a). We have observed an intriguing phenomenon: the methods inserted into shallow layers exhibit superior compatibility compared to those inserted into deep layers, despite the latter typically demonstrating better performance on downstream tasks. Remarkably, when these deep-layer methods are inserted into the updated model, their performance can even be lower than that of the zero-shot CLIP.

Why are shallow-layer methods superior to deep-layer ones? We delve deeper into the reasons why shallow-layer methods outperform deep-layer methods, investigating whether this superiority stems from the methods or the specific insertion positions. To begin with, as illustrated in Figure 2 (d), we conduct experiments by training the CoOp [Zhou et al., 2022b] across various layers of CLIP. The results reveal that, even when using the same method, the reused accuracy experiences a continuous decline with the deepening of layers, eventually falling below the zero-shot performance. The results align with deep-layer methods, indicating a correlation between the compatibility of the method and the layer at which it is integrated into CLIP. Subsequently, we analyze the differences in the text encoder of ViT-B/16-based CLIP and EVA-CLIP. In Figure 2 (b-c), we calculate the average absolute and relative changes in parameters and output features across different layers. The results reveal that, after the model upgrade, shallow layers exhibit smaller changes in parameters and output features compared to deep layers. This stability facilitates a smoother integration of modules into the updated model.

3.2 Class-conditioned Context Optimization

We propose a novel approach, **Class-conditioned Context Optimization (ContCoOp)**, designed for enhancing compatibility in VLMs. Our approach exhibits strong compatibility in the context of model upgrades within the VLMs across various datasets.

The design of our method is rooted in two key observations. 1) First, shallow-layer methods exhibit superior compatibility in upgraded VLMs. Thus, following previous works [Zhou et al., 2022b,a, Yao et al., 2023, Wang et al., 2023], we integrate learnable prompts at the initial layer of the text encoder in VLMs rather than designing modules at deeper layers of the model. 2) After upgrades, there is an improvement in the model’s zero-shot performance. Consequently, we posit that by leveraging zero-shot prompts as conditions, our method can dynamically adapt to model updates (due to zero-shot prompts embedding

change with the model updates). Since our approach stands on the shoulder of zero-shot prompts, it should yield superior compatibility.

The overview of our method is shown in Figure 3. We provide a detailed description of our approach below. Formally, let $\{w_i(P_i)\}_{i=1}^C$ represents the classifier weights generated by the text encoder where $w_i(P_i) = T(P_i), i = 1, \dots, C$. Here, C signifies the number of classes. The prompt embedding is represented by $P_i = [p, c_i] \in \mathbb{R}^{(N+1) \times D}$, where c_i corresponds to the embedding of the i -th class name, and $p = [p_1, \dots, p_N] \in \mathbb{R}^{N \times D}$ denote the learnable prompts within the embedding space.

To enhance the compatibility of our method, we design class-conditioned prompts as $p_i(c) = p_i + \text{Attn}(p, c), i = 1, \dots, N$. Here, c is the class embedding and Attn denotes the attention network, which fuses the class information into prompts through the following process:

$$\begin{aligned} Q &= XW_Q, \quad K = XW_K, \quad V = XW_V, \\ O &= \text{Softmax}\left(\frac{QK^T}{\sqrt{D}}\right)VW_O. \end{aligned} \quad (1)$$

Here, $X = [p, c] \in \mathbb{R}^{(N+1) \times D}$. The projection weights W_Q, W_K, W_V , and W_O correspond to query, key, value, and output, respectively, in line with standard attention networks. After fusion, we extract the output prompts as $\text{Attn}(p, c) = O[:N] \in \mathbb{R}^{N \times D}$. Subsequently, these class-conditioned prompts of each class, $p(c_i) = p + \text{Attn}(p, c_i)$, are fed into the text encoder to generate the final classifier, i.e., $w_i = T([p(c_i), c_i])$. Therefore, the classification probability can be computed as follows:

$$p(y = i|x) = \frac{\exp(\cos(w_i, f)/\tau)}{\sum_{j=1}^C \exp(\cos(w_j, f)/\tau)}, \quad (2)$$

where $f = I(x)$ is the image feature, and $\tau = 0.01$ is the temperature coefficient, and $\cos(\cdot, \cdot)$ denotes the cosine similarity. Furthermore, if we have a zero-shot classifier, we employ the knowledge distillation loss L_{kd} to fuse its knowledge into the learnable prompts as in [Yao et al., 2023],

$$L_{kd} = \frac{1}{C} \sum_{i=1}^C \|w_i - w_{zs,i}\|_2, \quad (3)$$

where $w_{zs} \in \mathbb{R}^{C \times D}$ is the zero-shot classifier. This approach differs from deep-layer methods, as it integrates the knowledge into the input prompts in the shallow layer, enhancing its compatibility rather than simply ensembling two classifiers. During fine-tuning, we maintain the VLM froze and optimize the learnable prompts and the attention network, guided by the loss function:

$$L = L_{ce} + \lambda L_{kd}, \quad (4)$$

where L_{ce} is the cross-entropy loss, and λ is a hyper-parameter to control the strength of L_{kd} .

4 Experiments

4.1 Setup

Datasets. In accordance with previous works [Radford et al., 2021, Zhou et al., 2022b,a, Wang et al., 2023], we conduct the experiments across 11 publicly available datasets, encompassing a diverse set of image recognition tasks. These tasks include generic object recognition using ImageNet [Deng et al., 2009] and Caltech101 [Li et al., 2004], fine-grained image recognition with OxfordPets [Parkhi et al., 2012], StanfordCars [Krause et al., 2013], Flowers102 [Nilsback and Zisserman, 2008], Food101 [Bossard et al., 2014], and FGVC Aircraft [Maji et al., 2013]. Additionally, we explored satellite image classification through EuroSAT [Helber et al., 2019], action classification with UCF101 [Soomro et al., 2012], texture classification

Table 1: Detailed statistics of datasets used in experiments.

Dataset	# Classes	# Training	# Test	Task
OxfordPets	37	2,944	3,669	fine-grained pets recognition
Flowers102	102	4,093	2,463	fine-grained flowers recognition
FGVCAircraft	100	3,334	3,333	fine-grained aircraft recognition
DTD	47	2,820	1,692	Textural recognition
EuroSAT	10	13,500	8,100	Satellite image recognition
StanfordCars	196	6,509	8,041	Fine-grained car recognition
Food101	101	50,500	30,300	Fine-grained food recognition
Sun397	397	15,880	19,850	Scene recognition
Caltech101	100	4,128	2,465	Object recognition
UCF101	101	7,639	3,783	Action recognition
ImageNet	1,000	1.28M	50,000	Object recognition
ImageNetV2	1,000	-	10,000	Robustness of collocation
ImageNet-Sketch	1,000	-	50,889	Robustness of sketch domain
ImageNet-A	200	-	7,500	Robustness of adversarial
ImageNet-R	200	-	30,000	Robustness of rendition styles

using DTD [Cimpoi et al., 2014], and scene recognition with SUN397 [Xiao et al., 2010]. To assess the out-of-distribution generalization of our method, we further include four datasets: ImageNetV2 [Recht et al., 2019], ImageNet-Sketch [Wang et al., 2019], ImageNet-A [Hendrycks et al., 2021b], and ImageNet-R [Hendrycks et al., 2021a].

Training Details. To assess the module compatibility with upgraded models in vision-language models, we utilize ViT-B/16-based CLIP by default. We train the plug-in modules on CLIP [Radford et al., 2021] and straightforwardly integrate them into its corresponding upgraded model, EVA-CLIP [Sun et al., 2023]. The length of prompts is set to 16 by default. The attention network is composed of a single multi-head attention layer with only one head, whose parameters are initialized using the Kaiming initialization method [He et al., 2015]. The hyper-parameter λ is set to 1.0 by default. All experiments are conducted on a single NVIDIA GeForce RTX 3090. To obtain a reliable estimate of model performance, we conduct three runs with different random seeds and average the results.

Evaluation Protocol. For module compatibility for upgraded models, we randomly select 16 samples for each dataset and train the models with 16-shot datasets using CLIP [Radford et al., 2021]. Subsequently, we assess the performance on the full test dataset using both CLIP and EVA-CLIP. The reported metric is the mean accuracy of the test dataset. In this context, we denote the performance achieved with CLIP as the base accuracy, while the performance with EVA-CLIP is considered the new accuracy. The harmonic mean of these two metrics is then reported as the trade-off between base and new accuracy.

4.2 Main Results

In this part, we present our approach and the performance of seven baselines under the module compatibility setting of VLMs. All methods are trained on 16-shot datasets using the ViT-B/16 CLIP.

Baselines. We evaluate our proposed approach against seven baseline methods for comparison: 1) **Zero-Shot CLIP** [Radford et al., 2021]: In the Zero-Shot CLIP (ZS-CLIP) baseline, we employ a prompt template such as "a photo of a [class]" to create a zero-shot classifier, assessing its reusability. 2) **Linear Probe** [Radford et al., 2021]: Following CLIP [Radford et al., 2021], we train a linear classifier on top of the pre-trained CLIP image encoder. 3) **CLIP-Adapter** [Gao et al., 2023]: CLIP-Adapter (CLIP-A) proposes to train a task-specific adapter to adjust the visual representations. 4) **Tip-Adapter-F** [Zhang et al., 2022]: Tip-Adapter-F (Tip-A) utilizes a cache of training data to construct the adapter, followed by fine-tuning on downstream tasks. 5) **CoOp** [Zhou et al., 2022b]: CoOp proposes learning context prompts for the input of the text encoder in downstream

Table 2: **Results in the module compatibility setting on 11 datasets.** We train these efficient modules using the ViT-B/16-based CLIP on 16-shot datasets. Subsequently, we directly integrate them into the corresponding version of EVA-CLIP. For comparison, we selected seven baselines: zero-shot CLIP, Linear Probe, CLIP-Adapter, Tip-Adapter, CoOp, CoCoOp, and KgCoOp. The evaluation metrics include the mean average of the dataset using both the original model (Base) and the upgraded model (New), along with their harmonic mean (H).

Dataset		ZS-CLIP	LP	CLIP-A	Tip-A	CoOp	CoCoOp	KgCoOp	ContCoOp
Average over 11 datasets	Base	65.51	78.15	79.56	81.63	79.94	76.27	78.30	81.27 (-0.36)
	New	70.79	1.83	67.30	69.63	75.40	75.39	<u>75.77</u>	79.32 (+3.57)
	H	68.04	3.57	72.92	75.15	<u>77.60</u>	75.83	77.01	80.28 (+2.68)
ImageNet	Base	68.80	58.16	70.90	73.73	71.62	71.52	71.04	<u>73.12</u>
	New	74.77	0.09	62.08	74.52	75.08	<u>75.86</u>	75.65	76.50
	H	71.66	0.18	66.18	<u>74.12</u>	73.31	73.63	73.27	74.77
Caltech101	Base	93.31	95.40	<u>95.92</u>	95.86	95.48	95.08	95.29	96.06
	New	97.16	0.54	96.15	96.62	96.74	97.34	<u>97.37</u>	97.51
	H	95.19	1.08	96.03	96.24	96.11	96.19	<u>96.33</u>	96.78
OxfordPets	Base	89.04	88.09	92.18	<u>92.87</u>	91.21	92.38	93.19	92.63
	New	92.23	2.96	89.35	91.94	91.09	<u>92.92</u>	93.17	92.45
	H	90.61	5.72	90.74	92.40	91.15	<u>92.65</u>	93.18	92.54
StanfordCars	Base	65.51	80.53	79.77	<u>83.19</u>	82.84	76.60	76.17	84.16
	New	79.16	0.29	75.34	75.31	80.10	<u>81.74</u>	81.44	84.01
	H	71.69	0.57	77.49	79.03	<u>81.45</u>	79.08	78.72	84.08
Flowers102	Base	70.73	<u>97.74</u>	96.48	97.60	97.17	95.10	94.21	97.88
	New	75.80	0.96	73.99	74.73	90.23	<u>90.62</u>	87.18	96.43
	H	73.18	1.90	83.75	84.65	<u>93.57</u>	92.81	90.56	97.15
Food101	Base	85.90	83.22	86.09	87.44	84.18	86.74	87.23	<u>87.24</u>
	New	86.56	1.28	83.84	86.13	84.05	86.68	86.89	<u>86.84</u>
	H	86.23	2.51	84.94	86.78	84.11	86.71	87.06	<u>87.04</u>
FGVCAircraft	Base	24.81	<u>46.42</u>	40.90	47.83	44.42	37.64	37.34	42.89
	New	24.66	0.67	23.61	21.75	27.36	<u>30.45</u>	28.37	32.96
	H	24.74	1.32	29.93	29.86	<u>33.87</u>	33.66	32.24	37.28
SUN397	Base	62.56	69.69	74.78	76.55	74.01	73.97	73.70	<u>76.54</u>
	New	70.82	0.30	62.75	69.92	73.96	<u>75.40</u>	74.72	76.26
	H	66.44	0.59	68.23	73.08	73.99	<u>74.68</u>	74.21	76.40
DTD	Base	44.09	71.30	71.18	71.24	69.78	58.98	69.86	71.95
	New	50.18	1.77	47.91	49.41	65.41	59.40	67.81	72.08
	H	46.94	3.45	57.26	58.34	67.52	59.18	68.81	72.01
EuroSAT	Base	48.35	86.43	82.95	<u>86.87</u>	85.56	72.95	81.11	86.88
	New	58.16	10.02	58.57	56.71	<u>69.05</u>	63.99	64.95	77.17
	H	52.80	17.93	68.64	68.61	<u>76.42</u>	68.16	72.12	81.64
UCF101	Base	67.46	82.68	84.04	84.76	83.04	78.06	82.18	<u>84.62</u>
	New	69.15	1.23	66.67	68.86	<u>76.36</u>	74.93	75.87	80.32
	H	68.30	2.42	74.35	75.99	<u>79.56</u>	76.45	78.90	82.42

tasks through back-propagation. For comparison, we choose the best version of CoOp which has 16 learnable prompts. 6) **CoCoOp** [Zhou et al., 2022a]: CoCoOp, a variant of CoOp, employs a meta-net to fuse visual features into learnable prompts, addressing the base-to-new generalization problem. 7) **KgCoOp** [Yao et al.,

2023]: KgCoOp introduces a knowledge distillation loss to enhance CoOp’s generalization ability.

Results. Table 2 illustrates the performance of our method and the baselines within the context of the model upgrade scenario. For clarity, we highlight the highest achieved results in bold, while the second-highest results are underscored to provide a clear distinction. From the results, we notice that despite the deep-layer methods (LP, CLIP-A, Tip-A) have demonstrated superior performance on the original CLIP (Base), their compatibility diminishes significantly in the upgraded model, falling even below the performance of the zero-shot CLIP. Post the model upgrade, LP, CLIP-A, and Tip-A exhibit reductions of 68.96%, 3.49%, and 1.16%, respectively, when compared to the zero-shot CLIP. This observation underscores their inability to reuse in the updated model. In comparison with these baselines, our method outperforms, achieving the highest results on 9 out of 11 datasets when applied to the upgraded model. On average over 11 datasets, our method attains the highest results for New and H scores, yielding improvements of 3.57% and 2.68%, respectively. This underscores the effectiveness of our approach in the context of model upgrades.

4.3 Out-of-distribution Generalization

We further conduct experiments to assess the robustness of our method against out-of-distribution generalization. Specifically, we train our model utilizing the ViT-B/16-based CLIP on 16-shot ImageNet [Deng et al., 2009]. Subsequently, we transfer the model directly to target datasets, which included ImageNetV2 [Recht et al., 2019], ImageNet-Sketch [Wang et al., 2019], ImageNet-A [Hendrycks et al., 2021b], and ImageNet-R [Hendrycks et al., 2021a].

As presented in Table 3, we choose ZS-CLIP [Radford et al., 2021], CoOp [Zhou et al., 2022b], CoCoOp [Zhou et al., 2022a], and KgCoOp [Yao et al., 2023] for comparison. Our method achieves the highest results on average over the four target datasets. Specifically, our approach surpasses ZS-CLIP, CoOp, CoCoOp, and KgCoOp by 3.21%, 1.98%, 0.48%, and 0.12%, respectively, on average. These results underscore the superior efficacy of our model in addressing challenges related to out-of-distribution generalization and mitigating the risk of overfitting on the source dataset.

4.4 Different Architecture

To demonstrate the adaptability of our approach, we evaluated its compatibility with an alternative CLIP architecture. We train our method and the baseline methods on a large CLIP architecture, ViT-L/14-based CLIP. All the methods are trained under 16-shot datasets.

The detailed results are shown in Table 8. Similar to the results on ViT-B/16 architecture, our method achieves the highest results on New and H. In comparison to the second-highest performing method, our approach achieves a 0.45% increase on the New and a 1.03% increase on the H. The results demonstrate the effectiveness of our method across different CLIP architectures.

4.5 Ablation Study

Table 3: Results of out-of-distribution generalization.

Method	Source		Target				Avg.
	ImageNet	-V2	-Sketch	-A	-R		
ZS-CLIP	66.73	60.83	46.15	47.77	73.96	57.18	
CoOp	71.92	64.18	46.71	48.41	74.32	58.41	
CoCoOp	71.02	64.07	48.75	50.63	76.18	59.91	
KgCoOp	71.20	64.10	48.97	50.69	76.70	60.12	
ContCoOp	73.12	65.50	48.36	50.43	77.29	60.39	

Table 4: Ablation of the attention network and knowledge distillation loss in our approach on the DTD dataset.

Attn	KD	Base	New	H
✗	✗	69.78	65.41	67.52
✓	✗	70.27	69.09	69.67
✗	✓	70.63	65.88	68.15
✓	✓	71.95	72.08	72.01

Effectiveness of different components. Our method is composed of two pivot components: the attention network (Attn) and the knowledge distillation (KD) loss, compared with previous work CoOp. In this

part, we ablate the effectiveness of these components. The results are presented in Table 4, The results demonstrate that integrating the attention network and KD loss independently yields enhanced module reusability. Notably, it is observed that the advantages stemming from the attention network surpass those of KD, showcasing a more pronounced improvement. Furthermore, combining these two components produces the best performance, yielding the effectiveness of our method.

Impact of variable context lengths. We analyze the influence of varying context lengths for prompts in our proposed method, as illustrated in Figure 4. Our experiments involve training our model with context lengths of 4, 8, and 16 on the UCF101 dataset. Notably, our findings reveal that the prompt length has a negligible impact on the performance of our method. Given that a context length of 16 yielded the optimal results, we adopt a context length of 16 for training our method, ensuring the attainment of superior results.

Table 5: Results of ContCoOp with different λ .

λ	0.00	0.30	0.50	0.70	1.00
Base	83.66	84.80	84.62	84.88	85.19
New	79.26	79.77	80.32	79.90	80.18
H	81.40	72.21	82.42	82.31	82.61

Table 6: Results of our method with different heads.

#heads	1	2	4	8	16
Base	71.95	72.16	72.04	72.08	72.06
New	72.08	71.95	71.73	71.04	71.22
H	72.01	72.00	71.88	71.56	71.64

Table 7: Different condition information of our method.

	Base	New	H
[class]	71.95	72.08	72.01
a photo of a [class]	72.01	70.74	71.37
[class] texture	71.51	71.53	71.52

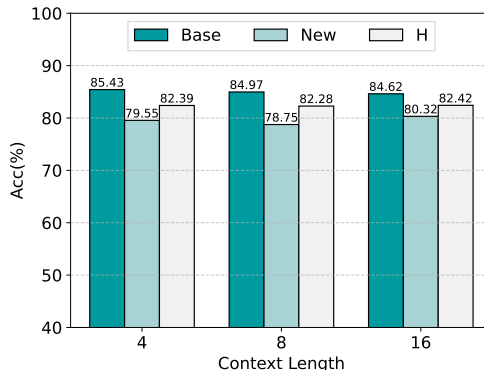


Figure 4: The impact of different context length.

Sensitivity analysis of the hyper-parameter λ . In our method, there is a hyper-parameter λ that controls the strength of knowledge distillation loss. To assess its impact, we conduct a sensitivity analysis on the UCF101 dataset. The results are shown in Table 5. We observe that the optimal performance is attained when λ is set to 1. Consequently, we adopt $\lambda = 1$ by default for all datasets.

Impact of varying the number of heads in the attention network. Our method incorporates an attention network with a self-attention layer. In this part, we explore the influence of adjusting the number of heads within the attention network. To assess the impact, we conducted experiments by training our model with varying numbers of heads on the DTD dataset. The results are shown in Table 6. The results indicate that employing a smaller number of attention heads yields better performance. Consequently, we opt to maintain a single head in the attention network.

Impact of conditional information. In ContCoOp, we leverage learnable prompts conditioned on class embeddings. However, it is noteworthy that our method allows for longer prompts as conditions, such as "a photo of a [class]". To ablate its influence, we train our method with different conditioned information on the DTD dataset. The results are shown in Table 7. Remarkably, our analysis reveals that opting exclusively for class embeddings as conditions yields the best results. This observation can be attributed to the embedding level, where prompts such as "a photo of a [class]" may lack significant semantic information. Due to the training methodology of CLIP, the semantic information of the prompt is primarily encoded in text features. Consequently, employing longer prompts introduces unnecessary noise during training, potentially hampering the performance.

Table 8: **Results in the module compatibility setting on ViT-L/14 architecture.** We train these efficient modules using the ViT-L/14-based CLIP on 16-shot datasets. Subsequently, we directly integrate them into the corresponding version of EVA-CLIP. For comparison, we selected seven baselines: zero-shot CLIP, Linear Probe, CLIP-Adapter, Tip-Adapter, CoOp, CoCoOp, and KgCoOp. The evaluation metrics include the mean average of the dataset using both the original model (Base) and the upgraded model (New), along with their harmonic mean (H).

Dataset		ZS-CLIP	LP	CLIP-A	Tip-A	CoOp	CoCoOp	KgCoOp	ContCoOp
Average	Base	72.76	82.74	84.86	85.90	84.66	83.71	83.61	<u>85.34</u> (-0.56)
	New	77.07	2.34	74.54	75.38	80.96	<u>82.47</u>	80.23	82.92 (+0.45)
	H	74.85	4.56	79.37	80.30	<u>82.77</u>	83.08	81.89	84.11 (+1.03)
ImageNet	Base	75.95	65.74	77.04	79.54	78.02	77.73	77.56	<u>78.99</u>
	New	79.88	0.10	71.33	79.62	80.07	<u>80.54</u>	80.44	81.04
	H	77.87	0.20	74.08	<u>79.58</u>	79.03	79.11	78.97	80.00
Caltech101	Base	95.17	96.92	97.40	97.69	97.23	97.19	<u>97.61</u>	97.55
	New	97.57	0.70	97.23	97.16	97.59	98.15	98.03	<u>98.07</u>
	H	96.35	1.40	97.32	97.42	97.41	97.67	97.82	<u>97.81</u>
OxfordPets	Base	93.43	92.01	94.48	94.85	93.99	<u>95.04</u>	95.10	94.62
	New	93.92	3.19	92.47	93.74	93.50	94.59	94.03	<u>94.11</u>
	H	93.68	6.15	93.46	94.29	93.74	94.81	<u>94.56</u>	94.37
StanfordCars	Base	76.84	85.74	87.55	<u>88.89</u>	88.77	86.02	84.54	89.43
	New	90.09	0.50	87.81	89.52	89.00	91.20	<u>90.88</u>	90.64
	H	82.94	1.00	87.68	<u>89.20</u>	88.88	88.53	87.60	90.03
Flowers102	Base	79.46	99.34	98.75	99.00	<u>99.04</u>	97.90	96.67	98.90
	New	77.22	0.84	77.44	70.42	<u>94.51</u>	93.00	85.93	94.94
	H	78.32	1.66	86.81	82.29	<u>96.72</u>	95.38	90.98	96.88
Food101	Base	90.91	89.47	91.13	91.82	90.10	91.22	<u>91.64</u>	91.61
	New	91.02	1.07	90.11	91.01	89.59	90.88	<u>91.33</u>	91.38
	H	90.97	2.12	90.62	91.41	89.84	91.05	<u>91.48</u>	91.49
FGVCAircraft	Base	32.61	55.92	55.94	59.48	<u>56.32</u>	51.65	49.78	53.88
	New	35.94	1.17	34.00	33.58	<u>44.04</u>	46.11	40.65	43.72
	H	34.20	2.29	42.29	42.91	49.38	48.72	44.75	<u>48.26</u>
SUN397	Base	67.66	72.36	78.34	79.72	77.26	77.40	77.04	<u>79.51</u>
	New	74.56	0.37	69.35	73.37	76.57	<u>78.53</u>	78.22	79.54
	H	70.94	0.74	73.57	76.41	76.91	<u>77.96</u>	77.63	79.53
DTD	Base	53.01	75.22	<u>75.67</u>	75.43	73.44	71.73	75.24	76.38
	New	63.36	2.52	57.96	61.54	69.70	<u>72.04</u>	70.55	74.55
	H	57.73	4.87	65.64	67.78	71.51	71.88	<u>72.81</u>	75.45
EuroSAT	Base	60.33	90.69	88.83	<u>90.48</u>	89.85	88.44	87.97	89.43
	New	67.43	14.21	66.64	62.74	73.42	<u>77.66</u>	71.95	78.94
	H	63.69	24.44	76.15	74.05	80.68	<u>82.67</u>	79.15	83.59
UCF101	Base	74.99	86.72	<u>88.38</u>	88.03	87.30	86.44	86.57	88.41
	New	76.79	1.11	75.54	76.46	82.62	<u>84.46</u>	80.56	85.20
	H	75.88	2.19	81.46	81.83	84.89	<u>85.44</u>	83.46	86.77

5 Conclusion

In this paper, we proposed a crucial issue in efficient fine-tuning for VLMs, i.e., *Are the efficient fine-tuned modules still effective to the upgraded model?* To investigate this, we first conducted experiments on the compatible performance of existing methods. The results revealed that, to varying degrees, these methods exhibit limitations in terms of compatibility. To address this issue, we proposed a novel approach, Class-

conditioned **Context Optimization (ContCoOp)**. ContCoOp generated the class-conditioned prompts through an attention network, thus the prompts can be dynamically updated for the upgraded model. We have conducted experiments over 15 datasets, illustrating the superior performance of ContCoOp. Moreover, ContCoOp not only demonstrated strong compatibility for model upgrades but also exhibited robust performance in out-of-distribution generalization. In the future, we plan to enhance our method and extend our research to explore the issue of compatibility in additional modalities, such as NLP.

Acknowledgments

This work was funded by the National Natural Science Foundation of China under Grant 62276256 and the Young Elite Scientists Sponsorship Program by CAST (2023QNRC001).

References

- L. Bossard, M. Guillaumin, and L. Van Gool. Food-101—mining discriminative components with random forests. In *ECCV*, 2014.
- T. Brown, B. Mann, N. Ryder, M. Subbiah, J. D. Kaplan, P. Dhariwal, A. Neelakantan, P. Shyam, G. Sastry, A. Askell, et al. Language models are few-shot learners. In *NeurIPS*, 2020.
- M. Caron, H. Touvron, I. Misra, H. Jégou, J. Mairal, P. Bojanowski, and A. Joulin. Emerging properties in self-supervised vision transformers. In *ICCV*, 2021.
- M. Cherti, R. Beaumont, R. Wightman, M. Wortsman, G. Ilharco, C. Gordon, C. Schuhmann, L. Schmidt, and J. Jitsev. Reproducible scaling laws for contrastive language-image learning. In *CVPR*, 2023.
- W.-L. Chiang, Z. Li, Z. Lin, Y. Sheng, Z. Wu, H. Zhang, L. Zheng, S. Zhuang, Y. Zhuang, J. E. Gonzalez, I. Stoica, and E. P. Xing. Vicuna: An open-source chatbot impressing gpt-4 with 90%* chatgpt quality, 2023. URL <https://lmsys.org/blog/2023-03-30-vicuna/>.
- M. Cimpoi, S. Maji, I. Kokkinos, S. Mohamed, and A. Vedaldi. Describing textures in the wild. In *CVPR*, 2014.
- J. Deng, W. Dong, R. Socher, L.-J. Li, K. Li, and L. Fei-Fei. Imagenet: A large-scale hierarchical image database. In *CVPR*, 2009.
- T. Dettmers, A. Pagnoni, A. Holtzman, and L. Zettlemoyer. Qlora: Efficient finetuning of quantized llms. *arXiv preprint arXiv:2305.14314*, 2023.
- P. Gao, S. Geng, R. Zhang, T. Ma, R. Fang, Y. Zhang, H. Li, and Y. Qiao. Clip-adapter: Better vision-language models with feature adapters. *IJCV*, 132(2):581–595, 2023.
- X. Gu, T.-Y. Lin, W. Kuo, and Y. Cui. Open-vocabulary object detection via vision and language knowledge distillation. In *ICLR*, 2021.
- K. He, X. Zhang, S. Ren, and J. Sun. Delving deep into rectifiers: Surpassing human-level performance on imagenet classification. In *ICCV*, 2015.
- P. Helber, B. Bischke, A. Dengel, and D. Borth. Eurosat: A novel dataset and deep learning benchmark for land use and land cover classification. *J-STARS*, 12(7):2217–2226, 2019.
- D. Hendrycks, S. Basart, N. Mu, S. Kadavath, F. Wang, E. Dorundo, R. Desai, T. Zhu, S. Parajuli, M. Guo, et al. The many faces of robustness: A critical analysis of out-of-distribution generalization. In *ICCV*, 2021a.
- D. Hendrycks, K. Zhao, S. Basart, J. Steinhardt, and D. Song. Natural adversarial examples. In *CVPR*, 2021b.

- N. Houlsby, A. Giurgiu, S. Jastrzebski, B. Morrone, Q. De Laroussilhe, A. Gesmundo, M. Attariyan, and S. Gelly. Parameter-efficient transfer learning for nlp. In *ICML*, 2019.
- E. J. Hu, P. Wallis, Z. Allen-Zhu, Y. Li, S. Wang, L. Wang, W. Chen, et al. Lora: Low-rank adaptation of large language models. In *ICLR*, 2022.
- C. Jia, Y. Yang, Y. Xia, Y.-T. Chen, Z. Parekh, H. Pham, Q. Le, Y.-H. Sung, Z. Li, and T. Duerig. Scaling up visual and vision-language representation learning with noisy text supervision. In *ICML*, 2021.
- K. Joseph, S. Khan, F. S. Khan, and V. N. Balasubramanian. Towards open world object detection. In *CVPR*, 2021.
- J. D. M.-W. C. Kenton and L. K. Toutanova. Bert: Pre-training of deep bidirectional transformers for language understanding. In *NAACL*, 2019.
- W. Kim, B. Son, and I. Kim. Vilt: Vision-and-language transformer without convolution or region supervision. In *ICML*, 2021.
- J. Krause, M. Stark, J. Deng, and L. Fei-Fei. 3d object representations for fine-grained categorization. In *ICCVW*, 2013.
- F.-F. Li, R. Fergus, and P. Perona. Learning generative visual models from few training examples: An incremental bayesian approach tested on 101 object categories. In *CVPRW*, 2004.
- X. Li, Z. Wang, and C. Xie. An inverse scaling law for clip training. In *NeurIPS*, 2023.
- X. L. Li and P. Liang. Prefix-tuning: Optimizing continuous prompts for generation. In *ACL-IJCNLP*, 2021.
- F. Liang, B. Wu, X. Dai, K. Li, Y. Zhao, H. Zhang, P. Zhang, P. Vajda, and D. Marculescu. Open-vocabulary semantic segmentation with mask-adapted clip. In *CVPR*, 2023.
- H. Liu, C. Li, Q. Wu, and Y. J. Lee. Visual instruction tuning. In *NeurIPS*, 2023.
- J. Lu, D. Batra, D. Parikh, and S. Lee. Vilbert: Pretraining task-agnostic visiolinguistic representations for vision-and-language tasks. In *NeurIPS*, 2019.
- S. Maji, E. Rahtu, J. Kannala, M. Blaschko, and A. Vedaldi. Fine-grained visual classification of aircraft. *arXiv preprint arXiv:1306.5151*, 2013.
- M.-E. Nilsback and A. Zisserman. Automated flower classification over a large number of classes. In *ICVGIP*, 2008.
- L. Ouyang, J. Wu, X. Jiang, D. Almeida, C. Wainwright, P. Mishkin, C. Zhang, S. Agarwal, K. Slama, A. Ray, et al. Training language models to follow instructions with human feedback. In *NeurIPS*, 2022.
- O. M. Parkhi, A. Vedaldi, A. Zisserman, and C. Jawahar. Cats and dogs. In *CVPR*, 2012.
- A. Radford, J. W. Kim, C. Hallacy, A. Ramesh, G. Goh, S. Agarwal, G. Sastry, A. Askell, P. Mishkin, J. Clark, et al. Learning transferable visual models from natural language supervision. In *ICML*, 2021.
- A. Ramesh, M. Pavlov, G. Goh, S. Gray, C. Voss, A. Radford, M. Chen, and I. Sutskever. Zero-shot text-to-image generation. In *ICML*, 2021.
- A. Ramesh, P. Dhariwal, A. Nichol, C. Chu, and M. Chen. Hierarchical text-conditional image generation with clip latents. *arXiv preprint arXiv:2204.06125*, 2022.
- B. Recht, R. Roelofs, L. Schmidt, and V. Shankar. Do imagenet classifiers generalize to imagenet? In *ICML*, 2019.

- R. Rombach, A. Blattmann, D. Lorenz, P. Esser, and B. Ommer. High-resolution image synthesis with latent diffusion models. In *CVPR*, 2022.
- M. Shu, W. Nie, D.-A. Huang, Z. Yu, T. Goldstein, A. Anandkumar, and C. Xiao. Test-time prompt tuning for zero-shot generalization in vision-language models. In *NeurIPS*, 2022.
- K. Soomro, A. R. Zamir, and M. Shah. Ucf101: A dataset of 101 human actions classes from videos in the wild. *arXiv preprint arXiv:1212.0402*, 2012.
- W. Su, X. Zhu, Y. Cao, B. Li, L. Lu, F. Wei, and J. Dai. Vi-bert: Pre-training of generic visual-linguistic representations. In *ICLR*, 2019.
- Q. Sun, Y. Fang, L. Wu, X. Wang, and Y. Cao. Eva-clip: Improved training techniques for clip at scale. *arXiv preprint arXiv:2303.15389*, 2023.
- R. Taori, I. Gulrajani, T. Zhang, Y. Dubois, X. Li, C. Guestrin, P. Liang, and T. B. Hashimoto. Stanford alpaca: An instruction-following llama model. https://github.com/tatsu-lab/stanford_alpaca, 2023.
- H. Touvron, L. Martin, K. Stone, P. Albert, A. Almahairi, Y. Babaei, N. Bashlykov, S. Batra, P. Bhargava, S. Bhosale, et al. Llama 2: Open foundation and fine-tuned chat models. *arXiv preprint arXiv:2307.09288*, 2023.
- H. Wang, S. Ge, Z. Lipton, and E. P. Xing. Learning robust global representations by penalizing local predictive power. In *NeurIPS*, 2019.
- Z. Wang, J. Liang, R. He, N. Xu, Z. Wang, and T. Tan. Improving zero-shot generalization for clip with synthesized prompts. In *ICCV*, 2023.
- Z. Wang, J. Liang, L. Sheng, R. He, Z. Wang, and T. Tan. A hard-to-beat baseline for training-free clip-based adaptation. In *ICLR*, 2024.
- J. Xiao, J. Hays, K. A. Ehinger, A. Oliva, and A. Torralba. Sun database: Large-scale scene recognition from abbey to zoo. In *CVPR*, 2010.
- C. Xu, Q. Sun, K. Zheng, X. Geng, P. Zhao, J. Feng, C. Tao, and D. Jiang. Wizardlm: Empowering large language models to follow complex instructions. *arXiv preprint arXiv:2304.12244*, 2023.
- H. Yao, R. Zhang, and C. Xu. Visual-language prompt tuning with knowledge-guided context optimization. In *CVPR*, 2023.
- R. Zhang, W. Zhang, R. Fang, P. Gao, K. Li, J. Dai, Y. Qiao, and H. Li. Tip-adapter: Training-free adaption of clip for few-shot classification. In *ECCV*, 2022.
- K. Zhou, J. Yang, C. C. Loy, and Z. Liu. Conditional prompt learning for vision-language models. In *CVPR*, 2022a.
- K. Zhou, J. Yang, C. C. Loy, and Z. Liu. Learning to prompt for vision-language models. *IJCV*, 130(9): 2337–2348, 2022b.